

## 0.1 Type II Weyl semimetals

The conic section problem with the intersecting plane restricted to pass through the node of the cone is trivially seen to have two solutions: a point and two intersecting lines. Despite this, the possibility of a Weyl cone tilted beyond the Fermi level was never considered before Soluyanov et al. described this new class of Weyl semimetals in 2015. This now seemingly obvious possibility made an already rich field even more exciting, opening up for a wider range of novel and interesting effects. **add some concrete examples or cites**

In the case of massless fermions, the particle physics equivalent of the Weyl semimetal, such a tilt is not possible, due to the requirement of Lorentz invariance **add cite or explain**.

In condensed matter physics, however, this is not an issue, and it is indeed a real class of materials **cite examples**. We denote these types of materials Type-II Weyl semimetals, as opposed to Type-I. The transition between Type-I and Type-II is abrupt – the Fermi surface goes from a single point to two intersecting lines, in other words going from a zero dimensional to a one dimensional surface. **Make sure this is indeed a one dimensional surface**

**Make sure it is one dim also for the 3D case, quadric surface, not conic intersection**

Type-II also has electron and particle pockets at the Fermi level. While the density of states for a Type-I semimetal goes to zero as one approaches the Fermi level, this causes Type-II to have a finite density of states at the Fermi level. **End with something like: all in all this gives**

### 0.1.1 Hamiltonian

We will firstly consider a slightly more realistic toy model for a Weyl semimetal, with a parameter taking the system from a Type-I to a Type-II. This is instructive both in order to more intuitively see the origin of the terms causing the tilting of the Dirac cone, and also to see how two Dirac cones in the same Brillouin zone tilt in relation to each other. We will then continue by linearizing the model around the Weyl points, regaining the familiar form of a Dirac cone, with an additional anisotropy term causing the tilt.

Using the general time-reversal breaking model described by McCormick, Kimchi, and Trivedi we have

$$H(\mathbf{k}) = [(\cos k_x + \cos k_z - 2)m + 2t(\cos k_x - \cos k_0)]\sigma_1 - 2t \sin k_y \sigma_2 - 2t \sin k_z \sigma_3 + \gamma(\cos k_x - \cos k_0). \quad (0.1)$$

The model has Weyl nodes at  $\mathbf{K}' = (\pm k_0, 0, 0)$ , and the parameter  $\gamma$  controls the tilting of the emerging cones. A value of  $\gamma = 0$  gives no tilt, while for  $\gamma > |2t|$  the Type-II system emerges. Figure 2 shows the cross section  $k_y = 0$  of the eigenvalues of this system, as  $\gamma$  is gradually increased from 0 to 0.15 **verify numbers**. The  $\gamma$ -term “warps” the bands, and in the limit of Type-II the hole band crosses the Fermi level into positive energy, while the particle band crosses the Fermi level into negative energies. We call these hole and electron pockets, respectively.

Linearizing around the Weyl nodes reduces to the familiar expression of a Dirac cone

$$H(\mathbf{K}'^{\pm} + \mathbf{k}) \approx \mp 2t k_x \sin k_0 \sigma_1 - 2t(k_y \sigma_2 + k_z \sigma_3) \mp \gamma k_x \sin k_0 \sigma_0, \quad k_x, k_y, k_z \ll 1. \quad (0.2)$$

When the separation between the two nodes is  $\pi$ , i.e.  $k_0 = \pi/2$ , the linearized Hamiltonian of around the cone, is

$$H'(\mathbf{k}) = \mp 2tk_x\sigma_x - 2tk_y\sigma_y - 2tk_z\sigma_z \mp \gamma k_x. \quad (0.3)$$

However, as the two nodes are brought closer together, the effective Fermi velocity in the  $x$ -direction is rescaled, and the system is anisotropic even for no tilt ( $\gamma = 0$ ). The expression may be made even more clear by moving the sign  $\pm$ -sign into the tilt parameter  $\gamma$ . The Hamiltonian is invariant under a sign change of the first term, as the isotropic Dirac Hamiltonian is invariant under inversion. In the tilt-term, we move the sign dependence into  $\gamma$ , and the linearized model is

$$H'(\mathbf{k}) = -2t\mathbf{k}\boldsymbol{\sigma} - \gamma^\pm k_x, \quad (0.4)$$

where  $\gamma^\pm = \pm\gamma$  with the upper sign corresponding to the node at  $k_x = +k_0$  and the lower sign corresponds to the node at  $k_x = -k_0$ . As expected, we get two Dirac cones, tilting in opposite direction, but with the same amount.

**How does this affect the Berry curvature and Chern**

**Maybe prettier/more correct to invert  $k_y$  and  $k_z$ , as that would also give the opposite chiral**

The linearized model are accurate in describing low energy interactions around the Fermi level. For higher energies their validity falls apart, and more complex models are warranted. In our calculations the linear models is sufficient, and much easier to work with, and we will thus mainly consider the linear model from here on.

- gives rise to cones tilting opposite direction
- Linearized model valid for low energy interaction. For higher energy, the perfect cone model is not valid, as the cones does in fact touch.
- In this model, the hole pocket is “shared” between the two cones. There are also models with individual pockets (see [1])

### 0.1.2 Eigenstates and Landau levels

The eigenvalues of Type-II Weyl semimetal simple to find, and are not qualitatively different from those of Type-I, other than the appearance of particle and hole pockets at the Fermi level. We will also consider the Landau levels of these materials, which importantly are very different from Type-I. In fact, erroneous treatment of the Landau spectrum of Type-II semimetals caused the original paper describing Type-II materials to mistakenly assert that the chiral anomaly would not be present for certain directions of a background magnetic field [3][2].

Eigenstates, spin, berry, etc

The issue with the Landau level description is that for certain directions of the  $B$ -field, the levels break down and become imaginary. For Type-I materials, the description is valid for all directions of the  $B$ -field, but as the cone tip into a Type-II material, the description breaks down when the  $B$ -field and tilt direction are perpendicular [2], and

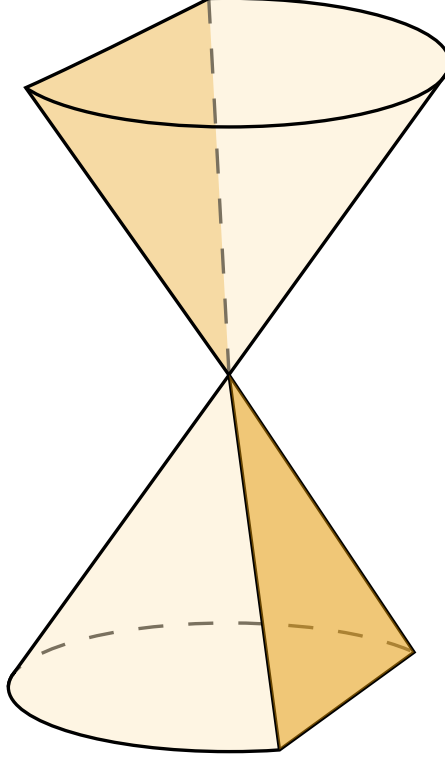


Figure 1:

as the magnitude of the tilt is increased, the Landau levels are only valid up to a certain angle between the tilt direction and magnetic field.

Consider the Hamiltonian

$$H = \boldsymbol{\omega}_0 \mathbf{k} + (\mathbf{v} \odot \mathbf{k}) \boldsymbol{\sigma}, \quad (0.5)$$

where  $\boldsymbol{\omega}_0$  is the tilt vector and  $\mathbf{v}$  is the Fermi velocity, which in general is anisotropic. To find the Landau levels in a magnetic field  $\mathbf{B} = B_z \hat{z}$ , we will “Lorentz boost” the system to a frame where the cone is not tilted, where we may use the usual approach for finding the Landau levels. Firstly, assume that the tilt vector  $\boldsymbol{\omega}_0$  is in the  $x, z$ -plane,  $\boldsymbol{\omega}_0 = (\omega_\perp, 0, \omega_\parallel)$ , which we can always achieve by a rotation around  $z$ . **Proof by figure** Introduce the  $\mathbf{B}$ -field by the minimal coupling  $\mathbf{k} \rightarrow \mathbf{q} = \mathbf{k} + e\mathbf{A}$ , and use the Landau gauge  $\mathbf{A} = -B_z y \hat{x}$ . The Hamiltonian can thus be written

$$H_B = \omega_\perp (k_x - eB_z y) + \omega_\parallel k_z + v_y k_y \sigma_y + v_z k_z \sigma_z + v_x (k_x - eB_z y) \sigma_x, \quad (0.6)$$

and the Landau level equation is

$$(H_B - E) |\psi\rangle = 0. \quad (0.7)$$

In order to use the ladder operator method used for the untilted cone, we must get rid of the  $q_x$  on the diagonal of the Hamiltonian. To achieve this, we will use a “Lorentz

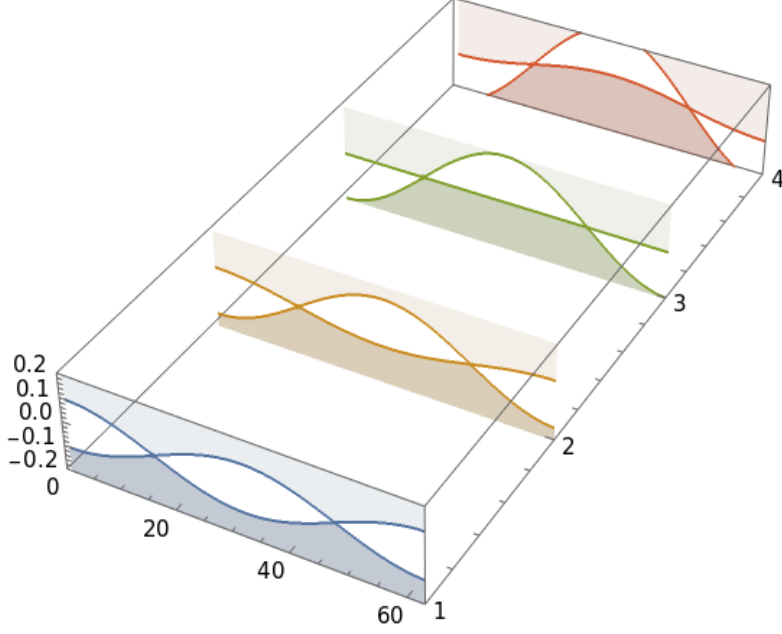


Figure 2: **Write this** The values of the parameters were chosen to be  $m = 0.15$ ,  $t = -0.05$ , and  $2k_0 = \pi$ .

transformation”, which as we will show only leave  $k_z$  and  $E$  in the diagonal. Act with the hyperbolic rotation operator  $\exp[\Theta/2\sigma_x]$  on Eq. (0.7), and insert identity on the form  $\exp[\Theta/2\sigma_x]\exp[-\Theta/2\sigma_x]$  before the state vector. By introducing the state in the rotate frame  $|\tilde{\psi}\rangle = \exp[-\Theta/2\sigma_x]\mathcal{N}|\psi\rangle$ , with  $\mathcal{N}$  a normalization factor compensating for the non-unitarity of the transformation, we get the eigenvalue equation

$$(\exp[\Theta/2\sigma_x]H_B\exp[\Theta/2\sigma_x] - E\exp[\Theta\sigma_x])|\tilde{\psi}\rangle. \quad (0.8)$$

We rewrite the Hamiltonian (Eq. (0.6)) in a more compact and explicit way

$$H_B = (\omega_\perp q_x + \omega_\parallel)\mathcal{I}_2 + \sum_i v_i q_i \sigma_i, \quad (0.9)$$

where  $\mathcal{I}_2$  is the identity matrix of size 2. We now make the fortunate observation that, with the hyperbolic rotation operator denoted  $R = \exp[\Theta/2\sigma_x]$ , the diagonal elements of

$$R\sigma_i R$$

are zero for  $i = y$  and non-zero for  $i = x, z$ . We may thus rotate the  $x$  and  $z$  in and out of the diagonal elements, without accidentally rotating the  $y$  components into the diagonal.

The problematic part of the Hamiltonian with regards to finding the Landau levels, are the terms containing  $q_x$  on the diagonal, i.e.

$$\omega_\perp q_x \mathcal{I}_2 + v_x q_x \sigma_x.$$

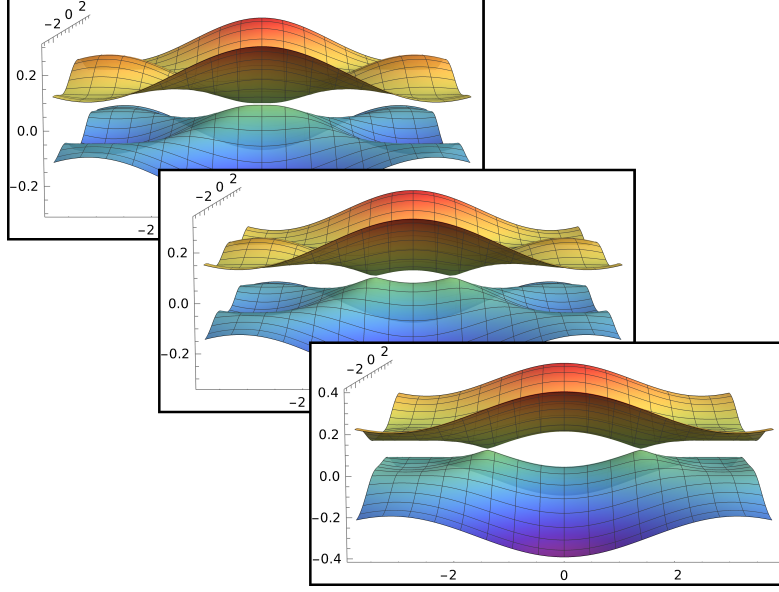


Figure 3: A Type-II Weyl semimetal with separation between the nodes  $2k_0 = 0, \pi/2, \pi$ . See main text for details about the model.

We will now find the boost parameter that eliminates  $q_x$  from the diagonal. We have

$$R^2 = e^{\Theta \sigma_x} = \begin{pmatrix} \cosh \theta & \sinh \theta \\ \sinh \theta & \cosh \theta \end{pmatrix} \quad (0.10)$$

and as  $[R, \sigma_x] = 0$ ,

$$R \sigma_x R = R^2 \sigma_x = \begin{pmatrix} \sinh \theta & \cosh \theta \\ \cosh \theta & \sinh \theta \end{pmatrix}, \quad (0.11)$$

as the effect of  $\sigma_x$  is to transpose the rows. The requirement for  $q_x$  to be rotated out of the diagonal is thus

$$\omega_{\perp} \cosh \theta + v_x \sinh \theta = 0. \quad (0.12)$$

Solving for  $\theta$  we get

$$\theta = \log(\pm \frac{\sqrt{v_x - \omega_{\perp}}}{\sqrt{v_x + \omega_{\perp}}}). \quad (0.13)$$

**NB: depending of choice of sign in log, we get different signs in answer** Alternatively, written in a slightly suggestive form,

$$\tanh \theta = -\frac{\omega_{\perp}}{v_x}. \quad (0.14)$$

**For pedagogic reasons, include arctanh, which is only valid for  $-1 \leq x \leq 1$ , explicitly showing**

Before we proceed any further, we will put the above into a more solid context, defining some useful quantities and more carefully investigate what is going on, which will be of help later when considering for the regions of validity, and the physical reason behind it.

**nice plot of the landau levels acutally being squeezed**

Introduce the dimensionless *tilt parameter*

$$\mathbf{t} = \left( \frac{\omega_{0x}}{v_x}, \frac{\omega_{0y}}{v_y}, \frac{\omega_{0z}}{v_z} \right).$$

Let also  $v_i = v_0 a_i$ , where  $\mathbf{a}$  is a vector describing the anisotropy of the system. In these parameters, the eigenvalues of the system are

$$E(\mathbf{k}) = \boldsymbol{\omega}_0 \mathbf{k} \pm \sqrt{(v_i k_i)^2} = \sqrt{(t_i v_i k_i)^2} \pm \sqrt{(v_i k_i)^2}. \quad (0.15)$$

The system is Type-II if the first term dominates for any  $\mathbf{k}$ , and Type-I if the last term dominates [3]. The  $\mathbf{t}$ -vector is thus a convenient tool for categorization – if  $t > 1$  we have a Type-II, else we have a Type-I.

*Proof.* We may always rotate our coordinate system such that, without loss of generality,  $\mathbf{t} = t\hat{x}$ . In that case, the first term obviously dominates in the  $x$ -direction, when  $t > 1$ .  $\square$

Expressed in the parameter  $t$ , the result in Eq. (0.14) has an intuitive, and quite visual, interpretation. As described above, we have rotated our frame such that the tilt is confined to the  $x, z$ -plane, i.e. no tilt in the  $y$ -direction. The required hyperbolic tilt angle to eliminate the  $q_x$  in the diagonal elements of the Hamiltonian, originating from the tilt, was

$$\theta = -\tanh^{-1} \frac{\omega_{\perp}}{v_x} = -\tanh^{-1} t_x. \quad (0.16)$$

The inverse of tan, of course, diverges as the argument approaches  $\pm 1$ , as shown in Figure 4. For  $t_x < 1$  we are able to find an angle  $\theta$  which transforms our Hamiltonian into a form

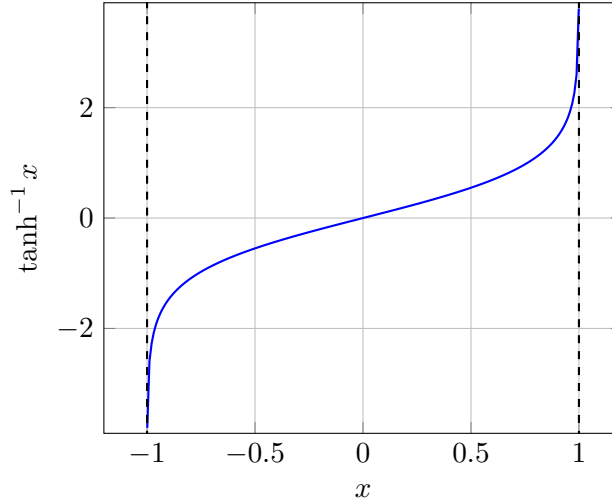


Figure 4: Plot of  $\tanh^{-1}$ , which diverges as the argument goes to  $\pm 1$ .

which we may solve. For  $t_x \geq 1$ , however, no (real) solution of  $\theta$  exists, and the Landau level description collapses. **Is this argumentation sufficient? What if we just have to use a different**

It is also interesting that there are no restrictions on the tilt in  $z, t_z$ . Visually, this can be visualized by plotting the  $t$ -vector inside a unit sphere. If the vector is outside the unit sphere, it is a Type-II, if it is inside, it is a Type-I. Also, if the projection of the vector onto the  $x, y$ -plane is on the unit disk, the Landau level description is valid, if not, the Landau levels collapse. All Type-I materials may thus be described by Landau levels, while it for Type-II is only valid for certain directions of the  $t$ -vector. As the  $t$ -vector gets larger, the region of valid directions is reduced to an ever smaller cone around  $z$ .

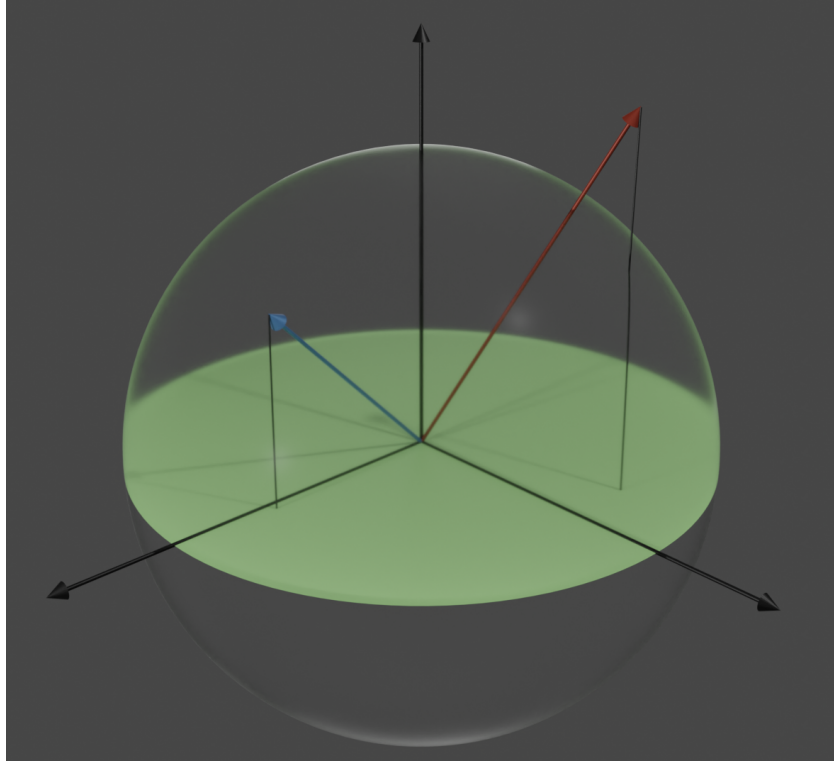


Figure 5: TODO

We now return to solving Eq. (0.8), using the solution angle we just found. By insertion, and after some clean up, we get *note to thorvald: we chose  $\theta = \text{Log}(+\dots)$*

$$= \begin{pmatrix} k_z(v_z + \omega_{\parallel}\gamma) - E\gamma & -ik_y v_y + \gamma q_x(v_x - \frac{\omega_{\perp}^2}{v_x}) + E\omega_{\perp}\gamma/v_x - k_z\omega_{\perp}\omega_{\parallel}\gamma/v_x \\ ik_y v_y + \gamma q_x(v_x - \frac{\omega_{\perp}^2}{v_x}) + E\omega_{\perp}\gamma/v_x - k_z\omega_{\perp}\omega_{\parallel}\gamma/v_x & -k_z(v_z - \omega_{\parallel}\gamma) - E\gamma \end{pmatrix} \quad (0.17)$$

after some more clean up

$$= \begin{pmatrix} k_z(v_z + \omega_{\parallel}\gamma) - E\gamma & -ik_y v_y + v_x q_x/\gamma - E\gamma\beta + k_z\omega_{\parallel}\gamma\beta \\ ik_y v_y + v_x q_x/\gamma - E\gamma\beta + k_z\omega_{\parallel}\gamma\beta & -k_z(v_z - \omega_{\parallel}\gamma) - E\gamma \end{pmatrix}. \quad (0.18)$$

Introducing  $\tilde{q}_x = q_x/\gamma + \gamma\beta\frac{k_z\omega_{\parallel}-E}{v_x}$  this may be further simplified as

$$\gamma(\omega_{\parallel}k_z - E)\mathcal{I}_2 + \tilde{q}_x v_x \sigma_x + q_y v_y \sigma_y + q_z v_z \sigma_z. \quad (0.19)$$

If we now again introduce the magnetic field using minimal coupling,  $q_x \rightarrow q_x - eyB_z$ , this corresponds to an effective field  $B_z/\gamma$  in the new quantities, as  $\tilde{q}_x \rightarrow \tilde{q}_x - eyB_z/\gamma$ . The Landau level equation thus reads

$$\left[ \sum_i v_i (\tilde{q}_i + eA_i) \sigma_i \right] |\tilde{\psi}\rangle = (E - \omega_{\parallel}k_z)\gamma |\tilde{\psi}\rangle, \quad (0.20)$$

where  $\tilde{q}_x = q_x, \tilde{q}_y = q_y, \mathbf{A} = -B_z/\gamma y \hat{x}$ . We may thus use directly the result for the untilted cone, **eq ref**, giving

$$(E - \omega_{\parallel}k_z) \gamma = \text{sign}(m)v_F \sqrt{2|m|e\frac{B}{\gamma}\hbar + k_z^2\hbar^2} \quad (0.21)$$

$$E = \omega_{\parallel}k_z + \text{sign}(m)v_F \sqrt{2|m|e\frac{B}{\gamma^3}\hbar + k_z^2\hbar^2/\gamma^2} \quad (0.22)$$

We may now use our previous solution Maybe use squeezing  $\alpha$  instead of  $\gamma$ ? **Fix anisotropic directions**

**Squeezing, etc**

We will boost the frame of the tilted cone such that the system is again isotropic, and use the well known solution for the Landau levels in that frame. The issue is that the boost is only valid for certain directions of the field. Add pretty figures describing the situation.



# Bibliography

- [1] Timothy M. McCormick, Itamar Kimchi, and Nandini Trivedi. “Minimal Models for Topological Weyl Semimetals”. In: *Phys. Rev. B* 95.7 (Feb. 21, 2017), p. 075133. DOI: 10.1103/PhysRevB.95.075133. URL: <https://link.aps.org/doi/10.1103/PhysRevB.95.075133> (visited on 02/08/2022).
- [2] Girish Sharma, Pallab Goswami, and Sumanta Tewari. “Chiral Anomaly and Longitudinal Magnetotransport in Type-II Weyl Semimetals”. In: *Phys. Rev. B* 96.4 (July 13, 2017), p. 045112. DOI: 10.1103/PhysRevB.96.045112. URL: <https://link.aps.org/doi/10.1103/PhysRevB.96.045112> (visited on 02/02/2022).
- [3] Alexey A. Soluyanov et al. “Type-II Weyl Semimetals”. In: *Nature* 527.7579 (7579 Nov. 2015), pp. 495–498. ISSN: 1476-4687. DOI: 10.1038/nature15768. URL: <https://www.nature.com/articles/nature15768> (visited on 01/24/2022).